sidebands are observed in YbGaG and 30 pairs in YbAlG. The remaining lines which cannot be so paired are identified as the electronic transitions between levels of the $^2F_{7/2}$ and $^2F_{5/2}$ groups. Using this information together with luminescent data it has been possible to identify for Yb^{3+} all the $^2F_{7/2}$ and $^2F_{5/2}$ energy levels, as summarized in Fig. 5.

The assignments differ most notably from previous assignments in that no $^2F_{7/2}$ states except the ground state are observed below 540 cm^{-1} in the gallium garnets and 600 cm^{-1} in the aluminum garnets. The significance of this observation will become more apparent in the discussion of magnetic susceptibilities to follow in II. In anticipation of these discussions, we note that Van Vleck,[9] arguing from susceptibility data alone, has already questioned the existence of electronic levels below the limits just set.

While it has been suggested that some Yb^{3+} ions may occupy sites other than the normal rare-earth site, we see no evidence for this in our YbGaG spectrum. Two extra lines were observed, however, in the YbAlG spectrum and on the basis of their intensities we conclude that a small percentage of the Yb^{3+} ions do occupy other than normal rare-earth sites in our aluminum garnet crystals. This observation, too, has some bearing on the susceptibility problem and will be discussed further in II.

Very weak Yb^{3+} emissions have been observed near 1.07 μ in YGaG and near 1.075 μ in YAlG. These emissions are thought to be transitions from the lowest $^2F_{5/2}$ electronic state to vibrational (overtone) levels near 975 cm^{-1} in YGaG and 1025 cm^{-1} in YAlG.

In closing, it should be emphasized once again that the level analyses presented here are now complete, unique, and independent of prior assumptions as to the crystal field. As such they provide (with separately determined g values for two states) a firm and sufficient basis for the crystal-field calculations to follow. The calculations in turn provide, through the quality of the fit, an independent verification of the experimentally deduced energy-level scheme. Beyond this, the calculations provide an unambiguous labeling of levels which could *not* have been obtained through experiment alone.

ACKNOWLEDGMENTS

It is a pleasure to acknowledge many helpful discussions with R. L. White. Without the exceptional garnet crystals grown by L. E. Sobon and F. A. Rogers this work would not have been possible. J. L. Weaver and E. E. Anderson also provided indispensable experimental assistance.

[9] J. H. Van Vleck, J. Phys. Chem. Solids **27**, 1047 (1966).

PHYSICAL REVIEW VOLUME 159, NUMBER 2 10 JULY 1967

Energy Levels of Yb^{3+} in Gallium and Aluminum Garnets. II. Calculations

J. J. Pearson. G. F. Herrmann, K. A. Wickersheim, and R. A. Buchanan

Lockheed Palo Alto Research Laboratory, Palo Alto, California

(Received 20 June 1966; revised manuscript received 14 November 1966)

Complete crystal-field calculations for Yb^{3+} in yttrium gallium and yttrium aluminum garnets have been performed. The energies and g values obtained in the ten-parameter fits agree well with experiment. The calculated crystal fields are predominantly cubic with important sixth-order contributions. A five-parameter fit to these data was also computed, using point-charge-model constraints derived by Hutchings and Wolf. Results indicate that the point-charge model is a useful first approximation, but too crude for quantitative predictions. On the basis of the derived wave functions, the susceptibility was calculated over a wide temperature range. For yttrium gallium garnet, results agree well with experiment, but for the aluminum garnet, the calculated temperature-independent susceptibility is appreciably below the reported value.

I. INTRODUCTION

In order to understand the magnetic properties of the rare-earth iron garnets on a microscopic basis it is helpful to be able to separate the effects on the rare-earth ion of the iron exchange and the diamagnetic lattice by replacing the latter with an effective crystal field. The parameters of this field can be obtained to a fair approximation from the energy levels of the rare-earth ion in structurally similar nonmagnetic garnets. The symmetry of the rare-earth site in the garnets is so low that no fewer than nine independent crystal-field parameters must be determined, and many pieces of experimental data are needed for an accurate calculation. An exact computer calculation is feasible, despite the low site symmetry, for a rare earth as electronically simple as trivalent ytterbium. Until now a complete calculation has not been carried out, partly because of the difficulty of the calculation and partly because of the scarcity of dependable experimental information. The paucity of f-electron energy levels for ytterbium forces the use of supplemental g-tensor information. Furthermore, the optical spectrum of ytterbium is surprisingly complicated, and an unambiguous assign-

ment of energy levels, particularly those of the lower ($J=\frac{7}{2}$) multiplet was not available.

In the most sophisticated and rigorous calculation to date, Hutchings and Wolf[1] (HW) avoided any utilization of the $J=\frac{7}{2}$ level spacings as input data. By calculating the electrostatic potential at the rare-earth site for a point charge crystal-field model, they were able to deduce constraints which effectively reduced the number of adjustable parameters to five. In this manner they were able to obtain a fair fit for the $J=\frac{5}{2}$ level separations and for the two known sets of g values. In addition the calculation yielded predicted values for the $J=\frac{7}{2}$ levels of Yb in yttrium gallium garnet (YGaG), namely, 517, 697, and 796 cm^{-1}.

In the meantime a complete experimental determination of the $J=\frac{7}{2}$ levels has been made, indicating that in fact these levels lie at 543, 599, and 642 cm^{-1}, in substantial disagreement with the HW prediction. An attempt, described below, to obtain the best simultaneous fit to all available data, using the point charge constraints, does not fare much better. This is not too disconcerting, since the point-charge model is admittedly a crude approximation. The question remains how good this approximation is when compared to a more general crystal-field solution.

Since twelve experimental values are now available, a determination of the ten adjustable parameters for Yb^{+++} is possible both in yttrium gallium and yttrium aluminum garnet (YAlG). A computer search program has been developed to obtain a best fit to the data. The result has been a generally good fit to the observed energy levels and g values. Because of the large number of parameters, considerable effort was expended in verifying the uniqueness of the solution and establishing the sensitivity of the fit to deviations of the parameters from their best values.

The parameters resulting from the general calculation are roughly similar to those of the HW-type calculation, the differences between the two sets of results lying typically between 30 and 60%. Both yield a predominantly cubic field and an unexpectedly high sixth-order crystal field. As already pointed out,[2] this forces a reidentification of the $J=\frac{7}{2}$ levels, with the Γ_6 doublet lying below the Γ_8 quartet.

We have performed a detailed calculation of the susceptibility in YbGaG and YbAlG using the calculated eigenfunctions. Results for the former agree well with experiment, but for the latter, the calculated temperature-independent susceptibility is somewhat too low. Possible sources of this discrepancy are discussed.

II. CRYSTAL-FIELD CALCULATION

Geometry

Before turning to the calculation itself, it is useful to define conventions. The first consideration is the choice of coordinate axes. The rare-earth ions in the garnet are located at 12 distinct sites which are related among themselves by the operations of the macroscopic octahedral symmetry group. The local site symmetry is orthorhombic (point group D_2) with one axis along a crystal [100] direction and the two others along appropriate [110] directions. In practice, since all calculations in this paper are invariant to the inversion operator we need to consider only six sites and a local symmetry of D_{2h}.

Each rare-earth ion is surrounded by eight oxygen ions, roughly at the corners of a cube (the so-called "pseudocube"). In the past, as well as in the present work, it has generally been assumed that the principal contribution to the crystal field possesses octahedral symmetry, and that a rough description of physical properties and the labeling of energy levels can be accomplished in terms of the octahedral symmetry group. This group is defined with respect to a system of local "pseudocubic" axes (xyz). There are three coordinate systems relevant to the problem: the unit-cell system (XYZ) with respect to which all macroscopic properties are defined, the system of orthorhombic local axes (x', y', z') which determine, for example, the principal directions for the g tensor, and the pseudocubic system (xyz) whose principal function is to make explicit the approximately cubic nature of the environment. Detailed transformations relating these coordinate systems are given in Appendix A.

Representation

In order to display the cubic parentage of the energy levels and distinguish clearly between cubic and noncubic components of the crystal field, basis functions and potentials were defined in terms of the irreducible representations of the octahedral group (see Appendix B). Although this constitutes no more than a formal change from past practice, it has brought to light features which remained hidden in the standard formulation using operator equivalents and $|JM_J\rangle$ basis functions. The functions in which we choose to expand the potential are the normalized tesseral harmonics described in detail in Appendix C, and for $4f$ basis functions the nine undetermined crystal-field parameters are the expansion coefficients of the field in terms of these harmonics. The $4f$ basis functions chosen reflect two features of the problem. First, that the spin-orbit coupling is so large for Yb^{3+} that J is nearly a good quantum number, and second, that the symmetry of the crystal site is approximately cubic. Thus, the $4f$ functions are first broken down into the ionic $^2F_{5/2}$ and $^2F_{7/2}$ multiplets and these are then decomposed into irreducible representations of the cubic double group. It should be emphasized, however, that this labeling scheme is employed primarily for display purposes and does not imply any additional approximations. The complete Hamiltonian is diagonalized in terms of the orthorhombic field.

[1] M. T. Hutchings and W. P. Wolf, J. Chem. Phys. **41**, 617 (1964).

[2] G. F. Herrmann, J. J. Pearson, and K. A. Wickersheim, J. Appl. Phys. **37**, 1312 (1966).

The Hamiltonian

The ground configuration of the free Yb^{+++} ion consists, outside of filled shells, of a single hole in the $4f$ shell. Since this case is formally identical to that of a single $4f$ electron (if the signs of the spin-orbit constant and of the crystal field are reversed), we will proceed as if we were dealing with the latter, conceptually simpler, situation. Conventional crystal-field theory assumes that the effect of placing the ion in the crystal can be approximated by applying to the free ion an electrostatic field having the same symmetry as the crystalline site. If configuration mixing is neglected (a good approximation for the free ytterbium ion), group theoretical considerations show that the most general such field for D_2 symmetry can be specified by nine parameters. The form chosen for the Hamiltonian in the present calculation is

$$H=\lambda\mathbf{L}\cdot\mathbf{S}+u_2^{\theta}U_2^{\theta}+u_2^{\zeta}U_2^{\zeta}+u_4^{a1}U_4^{a1}+u_4^{\theta}U_4^{\theta}+u_4^{\zeta}U_4^{\zeta}+u_6^{a1}U_6^{a1}+u_6^{\theta}U_6^{\theta}+u_6^{\zeta a}U_6^{\zeta a}+u_6^{\zeta b}U_6^{\zeta b}, \quad (1)$$

where the U's are tensor operators belonging to irreducible representations of the octahedral group (see Appendix C). No *a priori* assumptions are made concerning the coefficients. It is of some interest to contrast Eq. (1) with the standard Hamiltonian in crystal field theory,

$$H=\lambda\mathbf{L}\cdot\mathbf{S}+\alpha\langle r^2\rangle(A_2^0O_2^0+A_2^2O_2^2)+\beta\langle r^4\rangle(A_4^0O_4^0+A_4^2O_4^2+A_4^4O_4^4)+\gamma\langle r^6\rangle(A_6^0O_6^0+A_6^2O_6^2+A_6^4O_6^4+A_6^6O_6^6), \quad (2)$$

as applied, for example, in the HW point-charge calculation. Equation (2) implies a clear separation between those magnitudes, e.g., spin-orbit interaction and radial functions, which are properties of the ion, and the contribution of the crystalline environment in the form of an electrostatic potential. Thus, in the HW treatment, once the potential has been determined, fixed relations must obtain between coefficients of any given order. The crystal-field assumption is, however, a rather crude approximation even for the very well localized $4f$ shell, since the appropriate one-electron functions in the crystal are not the free-ion functions but molecular orbitals spanning the neighbor oxygens as well as the central ytterbium. In addition, the presence of shielding, and especially nonlinear shielding, introduces modifications in the potential which invalidate Eq. (2) in its strict formal sense.

On the other hand, the Hamiltonian as given in the more general form of Eq. (1) does not depend on the assumption that ionic $4f$ functions are being used, but only on the far less restrictive assumptions: (1) that the one-electron functions span the same irreducible representations of D_2 as do the $4f$ functions, and (2) that the spin-orbit interaction can be characterized by one parameter in the same way as it can for the ionic functions. Thus we can postulate that the functions we are using are actually molecular orbitals and realize that it is by no means true that we are neglecting covalency altogether. This postulate will not affect the details of the calculation but only the point of view adopted at certain stages of it. It explains, for example, why we do not assume the spin-orbit parameter to be the same as that for the free ion but instead allow it to vary along with the crystal-field parameters. It is also the reason why we expand the crystal potential in terms of purely angular functions, lumping all radial factors into the parameters to be determined, instead of attempting to draw any conclusions concerning their size from the radial dependence of the free-ion functions.

The Calculation

The first objective of the calculation is to determine the values of the coefficients u of Eq. (1) which will result in the best fit to the experimental data. For a given set of coefficients the energy levels and eigenfunctions are obtained by diagonalizing the 14×14 matrix which represents the Hamiltonian in the $4f$ configuration. In practice, the 14 functions can be divided into pairs of Kramers conjugates in such a way that the Hamiltonian separates into two identical 7×7 blocks. The spin-orbit interaction is diagonal and constant for all states of a given J. The Hamiltonian matrix for given crystal-field and spin-orbit parameters can then be constructed as a linear combination of the matrices for the individual U's and diagonalized to give the energy levels and wave functions. The wave functions are obtained as linear combinations of the basis functions with coefficients which are always real because of the orthorhombic symmetry.

We calculate g values in the usual way by calculating the magnetic moment in each Kramers doublet. In the present convention,

$$g_{x'}=-2((1+i)/\sqrt{2})\langle\psi\mid L_{x'}+2S_{x'}\mid\hat{\psi}\rangle,$$
$$g_{y'}=-2((1-i)/\sqrt{2})\langle\psi\mid L_{y'}+2S_{y'}\mid\hat{\psi}\rangle,$$
$$g_{z'}=-2\langle\psi\mid L_{z'}+2S_{z'}\mid\psi\rangle, \quad (3)$$

where $\mid\psi\rangle$ and $\mid\hat{\psi}\rangle$ represent a pair of Kramers conjugate wave functions associated with a given level. As defined, the g's are real but can be either positive or negative (see Appendix D).

The Computer Search Program

The calculation of the energies and g's in terms of known crystal field and spin-orbit parameters is perfectly straightforward. More complicated, however, is the inverse problem of determining the parameters from measured energies and g's. Algebraic inversion of the equations is out of the question, and in fact, uncertainties in the measurements and approximations in the theory make it highly unlikely, as the number of parameters increases, that an exact solution exists at all. Some form of sophisticated trial-and-error procedure of the type to which automatic computing

TABLE I. Energy levels (in cm^{-1}) and g values for Yb^{+++} in YGaG.

	Cubic only	Full fit	Exp	HW	Point charge
$J=\frac{5}{2}$					
$\Gamma_{8\mu}$	10 653	10 733	10 737±3	11 028	10 724
$\Gamma_{8\kappa}$	10 653	10 604	10 593±3	10 876	10 610
Γ_7	10 323	10 310	10 311±1	10 601	10 311
g^x	−1.48	−0.43	−0.35±0.1	−0.27	−0.10
g^y	−1.48	−2.28	−1.98±0.1	−2.14	−2.24
g^z	1.48	1.70	1.80±0.1	1.92	1.93
$J=\frac{7}{2}$					
$\Gamma_{8\mu}$	607	662	642±7	798	721
$\Gamma_{8\kappa}$	607	606	599±7	700	606
Γ_6	529	529	543±4	518	506
Γ_7	50	0	0	0	0
g^x	3.48	2.84	2.85±0.01	2.94	2.82
g^y	3.48	3.59	3.60±0.01	3.42	3.61
g^z	−3.48	−3.72	−3.73±0.01	−3.84	−3.82

machines are so well suited is called for. We have chosen to use the following least-squares approach.

A function S measuring the discrepancy between theory and experiment is defined by

$$S(P_1\cdots P_N)=\sum_i W_i[E_i(P_1\cdots P_N)-\bar{E}_i]^2, \quad (4)$$

where $P_1, \cdots, P_N$ are the parameters, E_i is a calculated energy or g value, $\bar{E}_i$ is the corresponding measured quantity, and W_i is an assigned weight. The problem reduces to that of minimizing the function S with respect to the ten P's. This was done using a numerical method due to Powell.[3]

This method is based on a property of second-order functions, namely, that a line through the minimum point of the function is the only one which cuts the level surface of the function at each point along the length of the line at the same angle. If one is able to find for each of two parallel planes in the n-dimensional-parameter space a point where the plane is tangent to a level surface of the function, then the straight line joining these two points passes through the minimum point of the function. (It cuts each of the two planes at the same angle at just those points where they are tangent to two level surfaces of the function.) The problem is then reduced to the one-dimensional one of minimizing the function along this line. Finding the two points which determine the line can be accomplished by the following procedure. The first point is taken to be the initial guess. The plane tangent to the level surface at this point is simply the plane normal to the gradient of the function at the point. Another point along this normal is then chosen (in practice it is the minimum point of the function along the normal) and a plane perpendicular to the normal (and hence parallel to the first plane) is constructed at this point. The point in this plane which we are seeking is one at which the plane is tangent to a level surface of the function. This will be true of the minimum point of the function in the plane. Finding this point is an $(N-1)$-dimensional problem in contrast to the original N-dimensional one. It is clear that by repeating this procedure, the problem is reduced to a one-dimensional one which can easily be solved.

Since the functional dependence of S on the P's is only approximately second order, the procedure must be repeated, but this iterative process converges quite well. Starting from an initial guess for the parameters it takes one to the nearest minimum of S. The minimum found by the initial fitting program is only rather crudely determined because, in the neighborhood of a minimum where first derivatives of S become small, roundoff error in the complicated machine calculation begins to dominate and the derivatives can no longer be calculated with any accuracy. The detailed behavior of S in the region near the minimum is of interest, however, because for a fit involving so many parameters, questions naturally arise about the uniqueness of the minimum and the accuracy with which the parameters are determined. Double precision arithmetic on the computer was therefore used to calculate S together with its first and second derivatives at the last point reached by the search program. Within the very small region including this point and the exact minimum, S is a quadratic function of the parameter increments to a high degree of approximation. Its minimum can therefore be found very accurately by extrapolating the first derivatives linearly to zero (occasionally a second iteration is required when the starting point is bad). S and its derivatives are then recalculated at the minimum. Use of this procedure yields several benefits. By determining the location of the minimum very accurately, one can verify that the minima reached from different initial guesses are really

[3] M. J. D. Powell, Comput. J. 5, 147 (1962).

the same and not closely spaced distinct minima. By diagonalizing the matrix comprised by the N^2 second derivatives at the minimum and verifying that its eigenvalues are all positive, one can verify that a true minimum, and not a saddle point, has been reached. Finally, the second derivatives permit one to establish limits on the accuracy with which each of the parameters is determined.

III. RESULTS

The experimental energies and principal g values which we chose to use as input to the fitting program, together with their estimated errors, are listed in Tables I and II. The sources of the energy levels are made clear in paper I. The g values for the ground state were obtained from paramagnetic resonance studies[4] and those for the excited state from Zeeman spectra.[5] It will be noted that the g values have signs

TABLE II. Energy levels (in cm^{-1}) and g values for Yb^{+++} in YGaG.

	Cubic only	Full fit	Experimental
$J=\frac{5}{2}$			
$\Gamma_8\,\mu$	10 634	10 678	10 674±3
$\Gamma_8\kappa$	10 634	10 623	10 620±3
Γ_7	10 334	10 321	10 322±1
g^x	−1.49	−0.51	−0.49±0.1
g^y	−1.49	−2.50	−2.46±0.1
g^z	1.49	1.47	1.27±0.1
$J=\frac{7}{2}$			
$\Gamma_8\kappa$	731	795	782±7
$\Gamma_8\,\mu$	731	688	696±7
Γ_6	542	604	611±4
Γ_7	104	0	0
g^x	3.49	2.47	2.47±0.01
g^y	3.49	3.77	3.78±0.01
g^z	−3.49	−3.86	−3.87±0.01

assigned to them. These signs are not given by the experiments from which the g's were obtained, but they are important to the calculation and were chosen according to the procedure discussed in Appendix D. The weights W_i in Eq. (4) were chosen in such a way that varying each quantity by its estimated experimental error would change S by the same amount.

Since with ten parameters to vary many different fits are possible, one must be careful to find that one which is the most reasonable physically. To assure this, three different sets of starting parameters, each obtained from plausible assumptions, were tried. They were: (1) best-fit parameters assuming the potential to be entirely cubic, (2) the HW parameters, (3) parameters resulting from a five-parameter best fit to *all* the available data, obtained by imposing the HW

[4] D. Boakes, G. Garton, D. Ryan, and W. P. Wolf, Proc. Phys. Soc. (London) **74**, 663 (1959); J. W. Carson and R. L. White, J. Appl. Phys. **31**, 53S (1960).
[5] H. M. Crosswhite (unpublished).

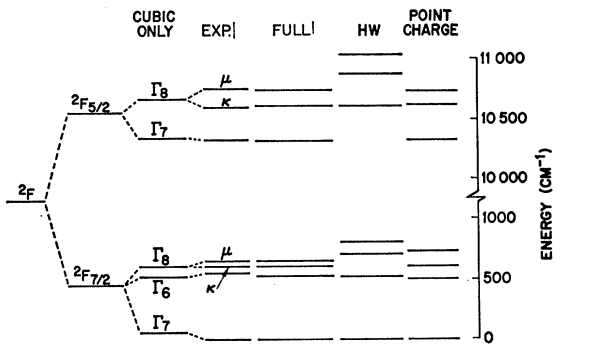

FIG. 1. Calculated and measured energy levels for Yb^{+++} in YGaG. The column "full fit" represents our best ten-parameter fit and corresponds to the potential coefficients given in Table III. The column "cubic only" represents a calculation using only the cubic crystal-field parameters u_4^{a1} and u_6^{a1} of Table III. The column HW shows the fit obtained by Hutchings and Wolf. (It should be noted that the HW fit is better than it appears here, since a large part of the discrepancy is due to an erroneously large spin-orbit parameter used by these authors.) The column "point charge" refers to a five-parameter fit to all the data using the point-charge ratios of Hutchings and Wolf. The data on which this figure is based are given in Table I.

point-charge ratios. (This last calculation, henceforth referred to as the "point-charge" fit, is interesting in its own right and will be discussed later.) From each of these starting points the ten-parameter search led to the same minimum. That it is a true minimum is confirmed by the positive signs of the eigenvalues of the second derivative matrix. In addition, the fact that the second derivatives change very slowly in the region of the minimum makes it highly unlikely that there is any other minimum nearby.

The results obtained are shown in Figs. 1 and 2 and in Tables I and II. Also shown are the results of the HW and point-charge calculations for the gallium garnet. The crystal-field parameters[6] corresponding to the energy levels and g's of Tables I and II are given in Table III. Estimates of the relative accuracies with

TABLE III. Crystal-field and spin-orbit parameters (in cm^{-1}) for the full fit, HW fit, and point-charge fit in the gallium garnet, and for the full fit in the aluminum garnet.

Parameter	Full fit (Al)	Full fit (Ga)	HW (Ga)	Point charge (Ga)
$\frac{7}{2}\lambda$	−9984± 4	−10 081± 6	−10 300	−10 068
u_2^θ	14±15	85±20	105	54
u_2^ζ	−249±12	−203±16	−210	−227
u_4^{a1}	−574±13	−610±19	−619	−592
u_4^θ	25±12	102±16	167	48
u_4^ζ	68±23	149±28	107	102
u_6^{a1}	−888±16	−647±26	−1 023	−836
u_6^θ	−314±22	−54±23	−50	−41
$u_6^{\zeta a}$	599±21	361±47	179	146
$u_6^{\zeta b}$	−121±18	−123±22	−123	−101

[6] For those who prefer to use the operator equivalents of Ref. 1, our full-fit parameters in terms of the A's of that paper are: For gallium, $A_2^0=-70$, $A_2^2=+288$, $A_4^0=-177$, $A_4^2=+221$, $A_4^4=+621$, $A_6^0=+49$, $A_6^2=-462$, $A_6^4=+822$, and $A_6^6=-233$; for aluminum, $A_2^0=-12$, $A_2^2=+352$, $A_4^0=-151$, $A_4^2=+102$, $A_4^4=+692$, $A_6^0=+107$, $A_6^2=-767$, $A_6^4=+1009$, and $A_6^6=-230$.

TABLE IV. Full-fit wave functions for the gallium garnet expanded in terms of the basis functions of Appendix B. The dominant cubic component of each wave function is given in boldface type.

State (energy in cm^{-1})	Coefficient of basis function						
	$\lvert\frac{7}{2}\Gamma_6\beta'\rangle$	$\lvert\frac{7}{2}\Gamma_8\mu\rangle$	$i\lvert\frac{7}{2}\Gamma_8\kappa\rangle$	$i\lvert\frac{7}{2}\Gamma_7\beta''\rangle$	$\lvert\frac{5}{2}\Gamma_8\mu\rangle$	$i\lvert\frac{5}{2}\Gamma_8\kappa$	$i\lvert\frac{5}{2}\Gamma_7\beta''\rangle$
10 733	−0.00252	0.00561	−0.00122	−0.00667	**−0.95697**	0.21226	0.19766
10 604	−0.00087	0.00638	−0.00406	−0.00290	0.19381	**0.97494**	−0.10897
10 310	0.00878	0.01709	−0.00576	−0.05088	−0.21518	−0.06623	**−0.97279**
662	−0.45246	**−0.85561**	0.16611	−0.18839	−0.00364	0.00496	−0.00978
606	0.38520	−0.06464	**0.90514**	0.16732	−0.00492	0.00478	−0.01100
529	**0.75974**	−0.50624	−0.38470	0.13582	−0.00589	0.00331	−0.00579
0	0.26385	0.08434	0.07130	**−0.95678**	0.01655	−0.00059	0.04986

which these parameters are determined are included as well. Figure 1 also indicates the way the free-ion energy level is split by terms in the Hamiltonian of successively lower symmetry: the spin-orbit interaction, the cubic part of the crystal field, and the full orthorhomic crystal field. It will be noted that the actual energy levels are labelled by the representations of the cubic group. That this is justified can be seen from Tables IV and V, where the expansion of the actual eigenfunctions in terms of the cubic basis functions is given. In every case, that cubic function which gives its name to an energy level predominates in the composition of the wave function corresponding to that level. Although the upper $J=\frac{7}{2}$ states are quite mixed, as expected from their close spacing, the more isolated states, including the two states for which g's are obtainable experimentally, are seen to be very strongly cubic. This well-defined cubic parentage of the eigenstates reflects the approximately cubic nature of the potential. As can be seen in Table III, the cubic terms, u_4^{a1} and u_6^{a1}, are significantly larger than the noncubic terms. (In contrast to the operator equivalents, the tensor operators used here are normalized quantities, and the coefficients give a true measure of the relative importance of the terms in the potential.) It can also be seen that the same labeling of the energy levels applies to the HW and point-charge calculations.

Examination of the point-charge fit reveals that the Hutchings-Wolf assumption of point-charge ratios among the fourth- and sixth-order parameters is not as inaccurate as one would be tempted to assume from the prediction for the $J=\frac{7}{2}$ levels given by the HW calculation. Instead, it gives a useful first approximation to the correct result. The signs of all the parameters agree, and their magnitudes are not grossly at variance.

A word should be said concerning the "error estimates" for the parameters quoted in Table II. For a multidimensional theoretical fit there can be no unique or truly satisfactory procedure for deriving such accuracy limits. We have chosen quite arbitrarily to define these limits in such a way that a change in a given parameter by an amount equal to its assigned error (all other parameters remaining fixed) will double the function S.

IV. SUSCEPTIBILITY

The magnetic moment induced at a particular ytterbium site by an applied magnetic field of any size can be calculated as a function of temperature by the rigorous formula

$$\mathbf{m}(\mathbf{H}) = [\sum_i \langle i \mid \boldsymbol{\mu} \mid i\rangle \exp(-E_i/kT)]/[\sum_i \exp(-E_i/kT)], \tag{5}$$

where

$$(H_{\text{crystal}}+H_{\text{spin-orbit}}-\boldsymbol{\mu}\cdot\mathbf{H}) \mid i\rangle = E_i \mid i\rangle, \tag{6}$$

and

$$\boldsymbol{\mu}=\beta(\mathbf{L}+2\mathbf{S}). \tag{7}$$

The eigenvalues E_i and eigenstates $\mid i\rangle$ are obtained by actually diagonalizing the Hamiltonian matrix in square brackets above within the 14-dimensional manifold of the $4f$ functions. For fields of the size normally attainable it is nearly as accurate to use the perturbation expansion of Eq. (5) to first order in H.

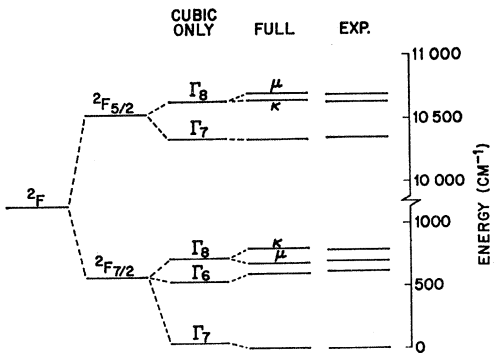

FIG. 2. Calculated and measured energy levels for Yb^{+++} in YAlG. This figure corresponds to the data in Table II.

TABLE V. Full-fit wave functions for the aluminum garnet. The dominant cubic component of each wave function is given in boldface type.

State (energy in cm^{-1})	$\lvert\frac{7}{2}\Gamma_6\beta'\rangle$	$\lvert\frac{7}{2}\Gamma_8\mu\rangle$	$i\lvert\frac{7}{2}\Gamma_8\kappa\rangle$	$i\lvert\frac{7}{2}\Gamma_7\beta''\rangle$	$\lvert\frac{5}{2}\Gamma_8\mu\rangle$	$i\lvert\frac{5}{2}\Gamma_8\kappa\rangle$	$i\lvert\frac{5}{2}\Gamma_7\beta''\rangle$
10 677	−0.00900	−0.01682	0.00646	0.01092	**0.96895**	0.01891	−0.24548
10 623	−0.00359	0.00563	−0.00579	−0.00170	−0.02247	**0.99963**	−0.01219
10 321	0.01980	0.02706	−0.01162	−0.06356	−0.24322	−0.01752	**−0.96708**
795	0.11011	0.44518	**−0.88809**	0.01300	0.01964	−0.00656	0.01971
688	−0.09524	**0.87928**	0.43185	0.17659	0.01039	−0.00222	0.00329
604	**0.92918**	−0.02341	0.10848	0.35247	0.00176	0.00466	−0.00663
0	0.33902	0.16461	0.11321	**−0.91665**	0.03141	0.00086	0.06252

Doing so yields the tensor relation

$$m_j(\mathbf{H}) = \sum_l H_l \left\{ \sum_i \exp\left(-\frac{E_{i0}}{kT}\right) \left[\frac{\langle i_0 \mid \mu_l \mid i_0\rangle\langle i_0 \mid \mu_j \mid i_0\rangle}{kT} + \sum_n \frac{\langle i_0 \mid \mu_l \mid n_0\rangle\langle n_0 \mid \mu_j \mid i_0\rangle + \text{c.c.}}{E_{n0} - E_{i0}} \right] \right\}$$
$$= \sum_l \chi_{jl} H_l, \tag{8}$$

where

$$(H_{\text{crystal}} + H_{\text{spin-orbit}}) \mid i_0\rangle = E_{i0} \mid i_0\rangle. \tag{9}$$

The macroscopic response to an applied field, obtained by summing Eq. (8) over all sites in the crystal, has the isotropic form

$$\mathbf{M} = \chi \mathbf{H}, \tag{10}$$

where

$$\chi = \tfrac{1}{3} N_0 \sum_i \chi_{ii}$$
$$= \left(\frac{N_0}{3 \sum_i \exp(-E_{i0}/kT)} \right) \sum_i \sum_j \exp(-E_{i0}/kT)$$
$$\times \left\{ \frac{\langle i_0 \mid \mu_j \mid i_0\rangle^2}{kT} + \sum_n \frac{2 \mid \langle i_0 \mid \mu_j \mid n_0\rangle \mid^2}{E_{n0} - E_{i0}} \right\}. \tag{11}$$

χ is defined as the gram-ionic susceptibility. One further observation can be drawn from this formula. If T is low enough so that $kT \ll [E_{i0} - E_1]$ for all $i \neq 1$ (E_1 is the ground-state energy), the factor $\exp(-E_i/kT)$ causes all terms except that with $i=1$ to become negligible. The temperature dependence of χ then has the form

$$\chi = C/T + \alpha, \tag{12}$$

with

$$C = (N_0/3k)[\langle 1 \mid \mu_x \mid 1\rangle^2 + \langle 1 \mid \mu_y \mid 1\rangle^2 + \langle 1 \mid \mu_z \mid 1\rangle^2], \tag{13}$$

and

$$\alpha = (2N_0/3) \times \sum_n \frac{\mid \langle 1 \mid \mu_x \mid n_0\rangle \mid^2 + \mid \langle 1 \mid \mu_y \mid n_0\rangle \mid^2 + \mid \langle 1 \mid \mu_z \mid n_0\rangle \mid^2}{E_{n0} - E_1}. \tag{14}$$

Deviations from this behavior would of course be expected at high temperature when the terms with $i \neq 1$ become important.

The applicability of the perturbation approximation leading to Eqs. (10) and (11) was tested by calculating the magnetization per gram ion by the rigorous formulas of Eq. (5) for a magnetic field of 10^4 Oe in various directions and for the temperature range 20–1000°K. $M(H)$ was found to exhibit isotropic behavior of the form (10) with χ given by Eq. (11) to within 0.06% over the entire range.

Susceptibilities for Yb^{+++} in the gallium and aluminum garnets have been measured by three different groups.[7–9] The results, expressed in terms of C and α [determined from the data in the range where Eq. (12) applies] are listed in Table VI, where they are compared with the values of these quantities calculated from Eqs. (13) and (14). The values for the gallium garnet are seen to lie well within the range of the experimental numbers. For the aluminum garnet there is some disagreement between the result of Ball *et al.*[7] for α and our calculation. These authors find almost identical values for α in both gallium and aluminum garnets, whereas the calculation predicts a considerable difference.

It should be emphasized that a discrepancy of this magnitude cannot be due to the detailed features of the calculation. Rather, it is a reflection of the fact that the energies which appear in the denominators of Eq. (14) are found experimentally to be quite different

[7] M. Ball, G. Garton, M. J. M. Leask, and W. P. Wolf, in *Proceedings of the Seventh International Conference on Low-Temperature Physics, 1960* (University of Toronto Press, Toronto, Canada, 1960), p. 128.
[8] Y. Ayant and J. Thomas, J. Cohen, and J. Ducloz, J. Phys. Radium **22**, 63S (1961).
[9] W. H. Brumage, C. C. Lin, and J. H. Van Vleck, Phys. Rev. **132**, 608 (1963).

TABLE VI. Experimental and theoretical susceptibility parameters [as defined in Eq. (12)] for YbGaG and YbAlG.

	Experimental			Theoretical
	Ref. 8	Ref. 7	Ref. 9	
Gallium				
C	1.09	1.116	1.082	1.089
α	0.003	0.00358	0.00397	0.00345
Aluminum				
C		1.111		1.100
α		0.00359		0.00272

in the two crystals. This is because the susceptibility depends only to second order on the noncubic potential terms,[10] as do the Γ_6 and mean Γ_8 energy levels.

Two possible explanations for the discrepancy suggest themselves: (a) The data of Ball *et al.*[7] obtained over a rather restricted range of low temperatures, is affected by exchange in a more complicated manner than is accounted for in the expression to which they fit their data; (b) The experimental susceptibility is modified by the presence of Yb on other than normal sites, evidence for which is adduced in Paper I.

[*Note added in proof*: Recent susceptibility measurements by C. C. Lin on the same YbAlG crystals used for the spectroscopy work of Paper I over the temperature range 77.3–905°K indicate a value for α of 0.0030. This agrees much better than the previous measurements with the theoretical result. We wish to thank Professor Lin for informing us of these measurements.]

The detailed temperature dependence of the susceptibility as calculated from Eq. (11), including its high-temperature bendover, is compared in Fig. 3 with the experimental points of Brumage *et al.*,[9] these being the only data available over the full temperature range of interest.

V. CONCLUSION

The search for a ten-parameter fit to the spectrum and g values resulted in a Hamiltonian dominated by its cubic terms. The Hamiltonian is thus consistent with the elementary picture, according to which the main contributions to the potential are the fourth- and sixth-order cubic terms due to the eight nearest-neighbor oxygens at the corners of the pseudocube surrounding the Yb^{+++} ion, the smaller noncubic terms arising from the displacement of the oxygens from ideal cubic positions and from more distant ions. The Hamiltonian is also in its rough features consistent with a point-charge model, although the latter is by itself insufficiently accurate for quantitative predictions (as shown by the failure of the original HW calculation properly to predict the remaining unknown levels). The fact that a unique solution is arrived at using either a cubic or a point-charge potential as starting points lends strong support to the belief that the calculated Hamiltonian is indeed the proper one. The Hamiltonian includes unexpectedly large sixth-order potential terms, forcing the Γ_8 levels of the $J=\frac{7}{2}$ manifold to lie above the Γ_6 levels contrary to what has been generally assumed in the past. These features are shared also by the approximate forms, i.e., the cubic, HW, and point-charge Hamiltonians.

It has been stated[11] that a tetragonal potential may represent a useful second approximation to the rare-earth potential in the garnets (a cubic potential representing the first approximation). No indication of tetragonal symmetry is given by our calculation, nor is it consistent with the point-charge model, or with the experimentally observed g values.

We believe that these calculations represent the most reasonable fits to the experimental data consistent with the assumptions we have made, the most important of which being that crystal-field theory is applicable and that only a single configuration need be considered. The failure of the calculation to fit all the experimental data within its limits of accuracy indicates that these assumptions are only approximately correct.

One of the purposes of the calculation was to obtain an approximation to the crystal-field parameters of ytterbium in the iron garnet. Since the iron and gallium garnets are structurally very similar, the iron garnet parameters should not differ much from the gallium parameters quoted here. Certainly the differences should be less than those between the gallium and aluminum garnet parameters. Finally, it should also

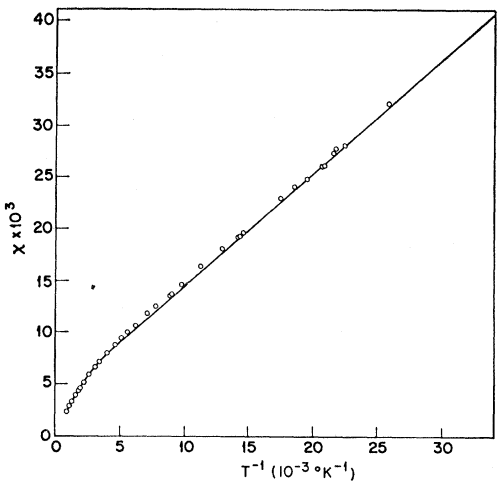

FIG. 3. Paramagnetic susceptibility per gram ion of Yb^{+++} in the gallium garnet calculated using our crystal-field parameters. The circles represent the susceptibility of YbGaG as measured by Brumage, Lin, and Van Vleck (see Ref. 2).

[10] This follows from the group-theoretical statement that functions with full cubic symmetry Γ_1 cannot depend linearly on functions belonging to Γ_i, $i \neq 1$. It is also borne out by the calculation, where the values of the squared matrix elements

$$\Sigma_j |\langle i_0 | \mu_j | n_0 \rangle|^2$$

for the orthorhombic wave functions were found to differ from those for the cubic wave functions by less than 10%.

[11] J. A. Koningstein, Theoret. Chim. Acta **3**, 271 (1965).

be emphasized that the data used in these calculations is for ytterbium dilutely doped into the garnets and that the crystal fields for the fully substituted garnets may be somewhat different. Comparison of the spectra in the two cases suggests, however, that these differences should not be large.

APPENDIX A: COORDINATE TRANSFORMATIONS

For a particular Yb^{3+} site the basis vectors for the orthorhombic coordinate system are given in terms of the crystal axes as follows:

$$\mathbf{n}_{x'}\equiv[1, 0, 0],$$
$$\mathbf{n}_{y'}\equiv[0, \tfrac{1}{2}\sqrt{2}, -\tfrac{1}{2}\sqrt{2}],$$
$$\mathbf{n}_{z'}\equiv[0, \tfrac{1}{2}\sqrt{2}, \tfrac{1}{2}\sqrt{2}].$$

The pseudocubic basis vectors for the same site are

$$\mathbf{n}_{x}\equiv[\tfrac{1}{2}\sqrt{2}, -\tfrac{1}{2}, \tfrac{1}{2}],$$
$$\mathbf{n}_{y}\equiv[\tfrac{1}{2}\sqrt{2}, \tfrac{1}{2}, -\tfrac{1}{2}],$$
$$\mathbf{n}_{z}\equiv[0, \tfrac{1}{2}\sqrt{2}, \tfrac{1}{2}\sqrt{2}].$$

Basis vectors for other sites are obtained by successive application of the operations of the crystal-symmetry group O.

Transformations among the coordinates are given by

$$\mathbf{x}'=\mathbf{X},$$
$$\mathbf{y}'=\tfrac{1}{2}\sqrt{2}(\mathbf{Y}-\mathbf{Z}),$$
$$\mathbf{z}'=\tfrac{1}{2}\sqrt{2}(\mathbf{Y}+\mathbf{Z}),$$

and

$$\mathbf{x}=\tfrac{1}{2}\sqrt{2}(\mathbf{x}'-\mathbf{y}'),$$
$$\mathbf{y}=\tfrac{1}{2}\sqrt{2}(\mathbf{x}'+\mathbf{y}'),$$
$$\mathbf{z}=\mathbf{z}'.$$

APPENDIX B: BASIS VECTORS

The basis vectors are of the form $|J\Gamma_i\gamma\rangle$ where γ denotes a particular row of a given representation Γ_i of the octahedral group O. We follow the notation and conventions of Griffith,[12] except for retaining the more popular designations Γ_6, Γ_7, and Γ_8 for the representations E', E'', and U', in the Griffith notation. Our basis functions, with proper phase, are given by

$$|\tfrac{7}{2}\Gamma_6\beta'\rangle,\ |\tfrac{7}{2}\Gamma_8\mu\rangle,\ i\,|\tfrac{7}{2}\Gamma_8\kappa\rangle,\ i\,|\tfrac{7}{2}\Gamma_7\beta''\rangle,$$
$$|\tfrac{5}{2}\Gamma_8\mu\rangle,\ i\,|\tfrac{5}{2}\Gamma_8\kappa\rangle,\ i\,|\tfrac{5}{2}\Gamma_7\beta''\rangle.$$

These seven functions together with their Kramers conjugates span the 14-dimensional eigenfunction space of the $4f$ configuration.

In terms of eigenfunctions of the form $|m_l m_s\rangle$ these functions are defined by

$$|\tfrac{7}{2}\Gamma_6\beta'\rangle=-[(\sqrt{5})/2\sqrt{3}]\,|3, \tfrac{1}{2}\rangle-(1/\sqrt{3})\,|0, -\tfrac{1}{2}\rangle-(\tfrac{1}{2})\,|-1, \tfrac{1}{2}\rangle,$$
$$|\tfrac{7}{2}\Gamma_8\mu\rangle=[(\sqrt{7})/2\sqrt{3}]\,|3, \tfrac{1}{2}\rangle-[(\sqrt{5})/\sqrt{21}]\,|0, -\tfrac{1}{2}\rangle-[(\sqrt{5})/2\sqrt{7}]\,|-1, \tfrac{1}{2}\rangle,$$
$$|\tfrac{7}{2}\Gamma_8\kappa\rangle=(\sqrt{3}/\sqrt{14})\,|2, -\tfrac{1}{2}\rangle+[(\sqrt{15})/2\sqrt{7}]\,|1, \tfrac{1}{2}\rangle+(\sqrt{3}/\sqrt{14})\,|-2, -\tfrac{1}{2}\rangle+(\tfrac{1}{2}\sqrt{7})\,|-3, \tfrac{1}{2}\rangle,$$
$$|\tfrac{7}{2}\Gamma_7\beta''\rangle=(1/\sqrt{14})\,|2, -\tfrac{1}{2}\rangle+[(\sqrt{5})/2\sqrt{7}]\,|1, \tfrac{1}{2}\rangle-(3/\sqrt{14})\,|-2, -\tfrac{1}{2}\rangle-(\sqrt{3}/2\sqrt{7})\,|-3, \tfrac{1}{2}\rangle,$$
$$|\tfrac{5}{2}\Gamma_8\mu\rangle=-(\sqrt{3}/\sqrt{7})\,|0, -\tfrac{1}{2}\rangle+(2/\sqrt{7})\,|-1, \tfrac{1}{2}\rangle,$$
$$|\tfrac{5}{2}\Gamma_8\kappa\rangle=-[(\sqrt{5})/\sqrt{42}]\,|2, -\tfrac{1}{2}\rangle+(1/\sqrt{21})\,|1, \tfrac{1}{2}\rangle-[(\sqrt{5})/\sqrt{42}]\,|-2, -\tfrac{1}{2}\rangle+[(\sqrt{5})/\sqrt{7}]\,|-3, \tfrac{1}{2}\rangle,$$
$$|\tfrac{5}{2}\Gamma_7\beta''\rangle=-(5/\sqrt{42})\,|2, -\tfrac{1}{2}\rangle+[(\sqrt{5})/\sqrt{21}]\,|1, \tfrac{1}{2}\rangle+(1/\sqrt{42})\,|-2, -\tfrac{1}{2}\rangle-(1/\sqrt{7})\,|-3, \tfrac{1}{2}\rangle.$$

The seven functions belong to the β ("spin-down") row of the representation $C_2{}^*$, associated with the two-fold symmetry axis along z. Functions $|\psi\rangle$ in the text refer to linear combinations of these spin-down functions, and functions $|\hat{\psi}\rangle$, to their Kramers conjugate spin-up functions.

APPENDIX C: DEFINITION OF OPERATORS AND CONVERSION FACTORS

The crystal-field Hamiltonian is expanded in terms of operators $U_l{}^{\Gamma\gamma}$ with transformation properties of Kubic harmonics of order l belonging to a row γ of a representation Γ of the octahedral symmetry group O. Only operators of orthorhombic symmetry and even l need to be included. For brevity we mark only the row of the representation using the notation of Griffith,[12] as the corresponding representation is always self-evident. The normalization is chosen expressly so as to make the norm of the matrices $U_l{}^{\gamma}$ within the $4f$ configuration equal to unity. The coefficients $u_l{}^{\gamma}$ in Eq. (1) therefore provide an absolute measure of the contribution of each term to the crystal-field splitting.

The most compact definition is given in an $|lm\rangle$

[12] J. S. Griffith, *The Theory of Transition Metal Ions* (Cambridge University Press, Cambridge, England, 1961).

representation, with quantization along z. The matrix elements are given by

$$\langle m \mid U_2^{\theta} \mid m' \rangle = (-1)^{m+1}\sqrt{5}\begin{pmatrix} 3 & 2 & 3 \\ -m & 0 & m' \end{pmatrix},$$

$$\langle m \mid U_2^{\zeta} \mid m' \rangle = -i(-1)^{m+1}\sqrt{5/2}\left[\begin{pmatrix} 3 & 2 & 3 \\ -m & 2 & m' \end{pmatrix} - \begin{pmatrix} 3 & 2 & 3 \\ -m' & 2 & m \end{pmatrix}\right],$$

$$\langle m \mid U_4^{a1} \mid m' \rangle = (-1)^{m+1}\left\{\tfrac{1}{2}\sqrt{21}\begin{pmatrix} 3 & 4 & 3 \\ -m & 0 & m' \end{pmatrix} + \frac{\sqrt{15}}{2\sqrt{2}}\left[\begin{pmatrix} 3 & 4 & 3 \\ -m & 4 & m' \end{pmatrix} + \begin{pmatrix} 3 & 4 & 3 \\ -m' & 4 & m \end{pmatrix}\right]\right\},$$

$$\langle m \mid U_4^{\theta} \mid m' \rangle = (-1)^{m+1}\left\{-\tfrac{1}{2}\sqrt{15}\begin{pmatrix} 3 & 4 & 3 \\ -m & 0 & m' \end{pmatrix} + \frac{\sqrt{21}}{2\sqrt{2}}\left[\begin{pmatrix} 3 & 4 & 3 \\ -m & 4 & m' \end{pmatrix} + \begin{pmatrix} 3 & 4 & 3 \\ -m' & 4 & m \end{pmatrix}\right]\right\},$$

$$\langle m \mid U_4^{\zeta} \mid m' \rangle = -i(-1)^{m+1}\frac{3}{\sqrt{2}}\left[\begin{pmatrix} 3 & 4 & 3 \\ -m & 2 & m' \end{pmatrix} - \begin{pmatrix} 3 & 4 & 3 \\ -m' & 2 & m \end{pmatrix}\right],$$

$$\langle m \mid U_6^{a1} \mid m' \rangle = (-1)^{m+1}\left\{\frac{\sqrt{13}}{2\sqrt{2}}\begin{pmatrix} 3 & 6 & 3 \\ -m & 0 & m' \end{pmatrix} - \tfrac{1}{4}\sqrt{91}\left[\begin{pmatrix} 3 & 6 & 3 \\ -m & 4 & m' \end{pmatrix} + \begin{pmatrix} 3 & 6 & 3 \\ -m' & 4 & m \end{pmatrix}\right]\right\},$$

$$\langle m \mid U_6^{\theta} \mid m' \rangle = (-1)^{m+1}\left\{\frac{\sqrt{91}}{2\sqrt{2}}\begin{pmatrix} 3 & 6 & 3 \\ -m & 0 & m' \end{pmatrix} + \tfrac{1}{4}\sqrt{13}\left[\begin{pmatrix} 3 & 6 & 3 \\ -m & 4 & m' \end{pmatrix} + \begin{pmatrix} 3 & 6 & 3 \\ -m' & 4 & m \end{pmatrix}\right]\right\},$$

$$\langle m \mid U_6^{\zeta a} \mid m' \rangle = -i(-1)^{m+1}\frac{\sqrt{13}}{\sqrt{2}}\left[\begin{pmatrix} 3 & 6 & 3 \\ -m & 2 & m' \end{pmatrix} - \begin{pmatrix} 3 & 6 & 3 \\ -m' & 2 & m \end{pmatrix}\right],$$

$$\langle m \mid U_6^{\zeta b} \mid m' \rangle = -i(-1)^{m+1}\frac{\sqrt{13}}{\sqrt{2}}\left[\begin{pmatrix} 3 & 6 & 3 \\ -m & 6 & m' \end{pmatrix} - \begin{pmatrix} 3 & 6 & 3 \\ -m' & 6 & m \end{pmatrix}\right],$$

where

$$\begin{pmatrix} l_1 & l_2 & l_3 \\ m_1 & m_2 & m_3 \end{pmatrix}$$

are Wigner $3j$ symbols.[13] From the properties of the $3j$ symbols one easily verifies the normalization

$$\sum_{mm'} \langle m \mid U_l^{\gamma} \mid m' \rangle \langle m' \mid U_{l'}^{\gamma'} \mid m \rangle = \delta_{\gamma\gamma'}\delta_{ll'}.$$

The same relation holds equally in any other representation.

The operators with full cubic symmetry are U_4^{a1} and U_6^{a1}.

The relation to spherical harmonics can be obtained from the equation[13]

$$\langle lm \mid Y_L^M \mid l'm' \rangle = (-1)^{l-m}\langle l \mid\mid Y_L \mid\mid l' \rangle \begin{pmatrix} l & L & l \\ -m & M & m' \end{pmatrix}.$$

[13] See, for example, M. Rotenberg, R. Bivins, N. Metropolis, and S. K. Wooten, Jr., *The 3-j and 6-j Symbols* (The Technology Press, Cambridge, Massachusetts, 1959).

The coefficients u_l^{γ} are related to the operator equivalent coefficients $A_l^m\langle r^l \rangle$, as used, e.g., in HW by the equations

$$u_2^{\theta} = -[(4\sqrt{7})/(5\sqrt{3})]A_2^0\langle r^2 \rangle,$$

$$u_2^{\zeta} = -[(4\sqrt{7})/15]A_2^2\langle r^2 \rangle,$$

$$u_4^{a1} = [4\sqrt{2}/3\sqrt{33}](7A_4^0 - A_4^4)\langle r^4 \rangle,$$

$$u_4^{\theta} = -[(4\sqrt{14})/(3\sqrt{165})](5A_4^0 + A_4^4)\langle r^4 \rangle,$$

$$u_4^{\zeta} = [(4\sqrt{14})/(3\sqrt{55})]A_4^2\langle r^4 \rangle,$$

$$u_6^{a1} = -[(40\sqrt{14})/(39\sqrt{33})](3A_6^0 + A_6^4)\langle r^6 \rangle,$$

$$u_6^{\theta} = -[40\sqrt{2}/39\sqrt{33}](21A_6^0 - A_6^4)\langle r^6 \rangle,$$

$$u_6^{\zeta a} = -[(32\sqrt{10})/(39\sqrt{11})]A_6^2\langle r^6 \rangle,$$

$$u_6^{\zeta b} = [160\sqrt{2}/429]A_6^6\langle r^6 \rangle.$$

APPENDIX D: SIGNS OF g VALUES

Measurements of magnetic splittings give no information about the signs of the principal values of the g tensor appearing in the spin Hamiltonian of paramag-

netic resonance, because the expressions for the splittings involve only the squares of the g values. In general, it is impossible to establish a unique correspondence between the two components of the actual Kramers doublet and the up and down states of the fictitious spin $\frac{1}{2}$ of the spin Hamiltonian, and it is therefore meaningless to talk about a sign for the g value. With the field along a symmetry axis, however, the transformation properties of the states allow each of them to be identified unambiguously with one of the spin components, and a sign for the g can then specify which of the two lies lower in energy.

When a magnetic field is applied along a twofold symmetry axis of the crystal site, the symmetry of the problem is reduced to that of the double group C_2^* around the axis in question. This new symmetry group is a subgroup of the original group as well as of the full-rotation group. C_2^* has only one-dimensional representations, and only two of these are allowed for odd-electron wave functions. Since a Kramers doublet transforms as a two-dimensional representation of the original group, its representation is reduced by the lowering of the symmetry, and one of the components of the split doublet transforms as each of the two possible representations of C_2^*, namely,

$$C_2^* \mid \psi\rangle = i \mid \psi\rangle,$$

$$C_2^* \mid \hat{\psi}\rangle = -i \mid \hat{\psi}\rangle,$$

where C_2^* is defined as a positive rotation of π about **H**. The wave function of a free spin quantized along the direction of the magnetic field also transforms as one of these representations, and that of a spin quantized opposite to the field transforms as the other. One can thus uniquely identify the two components of the split doublet by comparing their transformation properties with those of a free spin. A positive g value can then be assigned to the doublet if the energy of the state transforming as the plus spin is the higher in the magnetic field and a negative g if it is the lower. This convention is the one reflected in the signs of the g's given by Eq. (3).

It must be stressed that it is this possibility of labeling the two components of the split doublet uniquely, and, in principle at least, of distinguishing them experimentally, which makes the sign of the g value a meaningful concept. In turn, it is the presence of a symmetry axis in the direction of the field which makes such a labeling possible. In an arbitrary (nonsymmetry) direction a magnetic field removes all the symmetry of the site, and it makes no sense to talk about which of the split states lies higher, since they cannot be distinguished.

The magnitude of g is thus a well-defined continuous function of the direction of the field. The sign associated with g, however, is defined only along symmetry axes and can be different for different axes (as in the present case) even though g is not zero in any direction. In addition to the meaning given here for the signs of the individual principal g values, the sign of their product is involved in the relation between magnetic moment and angular momentum.[14]

Once it is established that the signs of the principal g values are meaningful (since the principal axes of the g tensor are indeed the twofold symmetry axes of the orthorhombic site), the practical problem of choosing them can be resolved by the following considerations. The g's and their signs are well defined for the cubic parents of the doublet states and are listed in the cubic columns of Tables I and II. Since one expects the actual eigenstates to resemble their cubic parents quite closely, it is reasonable to assume that the signs of the g's will be the same as they are for the cubic functions. Any other assumption forces the states artificially to be noncubic or to resemble cubic states of the wrong J. (Note that the Γ_7 state coming from $J=\frac{7}{2}$ has opposite signs for its g's from that coming from $J=\frac{5}{2}$.) Making the wrong choice of signs, or attempting to fit only the absolute values of the g's, greatly increases the chance of reaching a false minimum and obtaining an unrealistic fit. It should be pointed out that the signs obtained in this way agree with those used by Hutchings and Wolf.[1]

[14] M. H. L. Pryce, Phys. Rev. Letters **3**, 375 (1959).